Environmental Science & Technology

Article

pubs.acs.org/est

Surface-Enhanced Raman Spectroscopy: A Facile and Rapid Method for the Chemical Component Study of Individual Atmospheric Aerosol

Yu Fu,[†] Christian Kuppe,[‡] Ventsislav K. Valev,[‡] Hongbo Fu,[†] Liwu Zhang,*[,†] and Jianmin Chen[†]

[†]Shanghai Key Laboratory of Atmospheric Particle Pollution and Prevention, Department of Environmental Science & Engineering, Fudan University, Shanghai 200433, People's Republic of China

[‡]Centre for Photonics and Photonic Materials, Department of Physics, University of Bath, Claverton Down, Bath BA2 7AY, United Kingdom

Supporting Information

ABSTRACT: A simple and rapid method for detecting chemical components of individual aerosol particles on Klarite substrate with surface-enhanced Raman spectroscopy (SERS) is described. For both single simulated aerosol particles and ambient atmospheric particles, this new analytical method promotes the enhancement factor of the Raman signal. The spectra of ammonium sulfate and naphthalene particles at the microscopic level are enhanced by a factor of 6 and therefore greatly improve the detection of the chemical composition of an individual aerosol particle. When aerosol particles are found over a microscopic domain, a set of Raman spectra with chemical information can be obtained via SERS mapping. The maps illustrate the distribution of organic or inorganic species on the SERS substrate. This constitutes a facile and rapid method to study aerosol particles. This new method allows the analysis of chemical composition in single aerosol particles, demonstrating the power of SERS to probe the ambient atmospheric particles and to study the formation of aerosol particles.

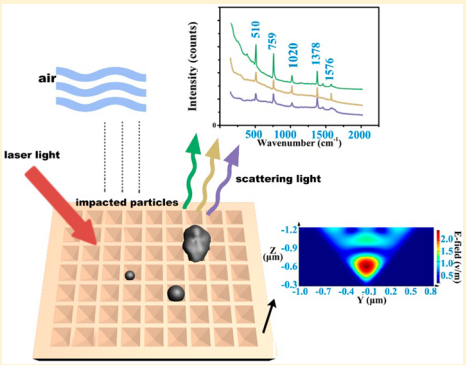

1. INTRODUCTION

Air pollution and its detrimental effects on the global environment and human health are topics of continuous interest. Both individual and bulk analysis of aerosol particles are of great importance to get a better understanding of the atmosphere's systems.[1] Various characteristics of aerosol, such as element composition, hygroscopicity, acidity, mixing state, etc., have an impact on cloud condensation nucleation (CCN), ice nucleation (IN) and, ultimately, the climate.[2−4] Among them, some of the first and most-crucial questions on aerosol particles are related to identifying the chemical composition. A single aerosol particle is the fundamental and original unit of larger aerosol particles, and it carries key chemical information, different from particle ensembles.[5] Therefore, there is an explicit need for the detection of trace chemical components in single aerosol particles.

Many single particle aerosol mass spectrometers were set in scientific research sites around the world to study the characteristics of individual particles, such as aerosol time-of-flight mass spectrometry (ATOFMS) and single-particle aerosol mass spectrometry (SPAMS), and work on a method of separating the charged particles and analyzing the ionized components of the particle.[6,7] Currently, many studies of single aerosol particles focus on nonintrusive methods with spatial and time resolution, often in the nano- or micrometer regime.[8,9] The techniques should have high chemical sensitivity and fast response time so that small changes in the properties of the individual particles can be detected or tracked. Raman spectroscopy is a nondestructive vibrational spectroscopy that has extensive applications in the detection of environmental pollutants. Especially in the field of atmospheric research, Raman spectroscopy has been proved to be useful for probing the properties of airborne particles at ambient temperature and pressure,[10] such as chemical composition, water solubility, phase transition, efficiency of light absorption, and so on. Raman spectroscopy was also applied to study the hygroscopic and phase-transition properties[11,12] as well as the heterogeneous reactivity of nitric acid with nascent sea spray aerosol.[13] In addition, Raman spectroscopy combined with other separation methods such as electrodynamic balance (EDB), optical tweezers,[14,15] and acoustic levitation have all been applied in the study of single aerosol particles. Raman tweezers and EDB have been reported to be able to trap an individual aerosol to explore the equilibrium properties of mixed component aqueous aerosol particles. With scanning trans-

Received: November 23, 2016
Revised: May 8, 2017
Accepted: May 12, 2017
Published: May 12, 2017

DOI: 10.1021/acs.est.6b05910
Environ. Sci. Technol. 2017, 51, 6260−6267

mission X-ray microscopy (STXM), Takahama et al. successfully measured organic functional group abundance and morphology of atmospheric aerosols.[16]

Surfaced-enhanced Raman spectroscopy (SERS) provides a drastic enhancement of the scattering efficiency over traditional Raman spectroscopy. SERS is primarily due to the presence of intense electromagnetic fields localized at the metal surface, where molecules are adsorbed.[17,18] By means of SERS, single aerosol particles on or near the surface of plasmonic nanostructures will attain enhanced factors up to 6 orders of magnitude and detection limits of tens of picograms.[19,20] To achieve a high enhancement factor, it is critical to gain large quantities of SERS-active "hotspots".[21] Therefore, the fabrication of effective and robust SERS substrates is of great importance,[22] and a variety of nanostructures, such as nanoflower,[23] nanorod arrays,[24] and nanowells[25] have been suggested. These nanostructures include many patterned metallic (usually Ag, Au, and Cu) substrates with nanoscale features.[26,27]

To the best of our knowledge, applications of SERS for atmospheric aerosol studies are very rare. Ayora et al.[28] first determined four different synthetic aerosol samples and realized the detection and quantitation of atmospheric pollutants in aerosols using SERS. Ault et al. first reported the use of SERS to investigate the previously undetectable secondary organic aerosol particles in remote forested regions through impacting aerosol particles on Ag nanoparticle-coated quartz substrates.[29] They compared the normal Raman and SERS-enhanced spectra of four different vibrational modes, $\nu(NO_3^-)$, ν(O−H), ν(C−H), and δ(C−C), and observed an enhancement for particles on SERS-active substrates. It is also demonstrated by Davis et al. that SERS is a powerful tool for bioaerosol characterization.[30,31] However, there are several shortcomings of using substrates such as Ag nanoparticle-coated quartz or colloidal suspensions of Ag nanoparticles. For example, low measurement reproducibility and low enhancement factor due to the lack of uniformity in the distribution of "hotspots". It is still a challenge to find a suitable substrate for atmospheric aerosol study.

Klarite is a commercial SERS substrate with an ordered structure of inverted pyramids. Klarite substrates are fabricated by vapor deposition techniques in which a thin gold layer is deposited on a silicon surface. The pyramid pits are produced by chemical etching of Si surfaces, determined on the basis of a mask designed by optical lithography. The inverted pyramids have a fixed apex angle (70.5° along the (111) direction of Si) and a scalable depth.

In this work, we use Klarite to focus the incident laser beam in the middle of the pit and obtain stable, high-intensity spectra, which provide rapid and qualitative information on individual aerosol particles. Klarite shows good measurement reproducibility and a high enhancement factor due to its uniform distribution of large quantities of "hotspots".[18,32] Moreover, the inverted pyramid structure is extremely suitable for aerosol particle sampling and analyzing (Figure 1). Although it has been widely studied in the field of food safety detection[33,34] and water pollution analysis,[35] there is no research focusing on using Klarite for atmospheric aerosol studies. We compared both inorganic and organic aerosol particles as well as ambient atmospheric aerosols on Klarite and silicon wafer. Subsequently, the enhancement of Raman scattering intensity for Klarite is demonstrated for both inorganic and organic components. A theoretical simulation has been carried out to understand the advantage of using Klarite as a SERS substrate for atmospheric aerosol characterization.

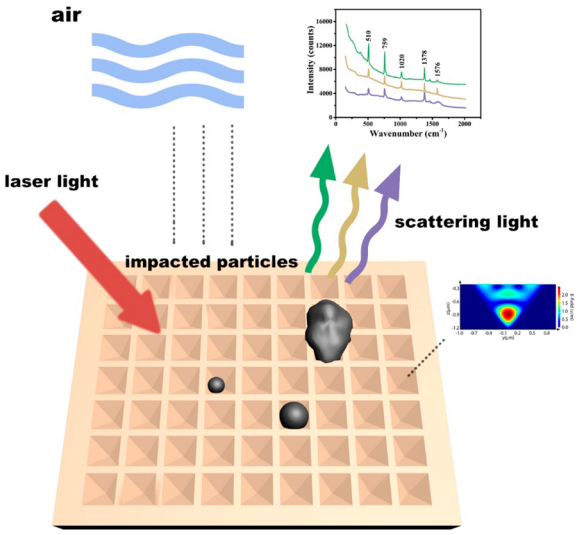

Figure 1. Schematic illustration of the use of Klarite to study aerosol particles via SERS.

2. EXPERIMENTAL SECTION

2.1. Sample Collection. Laboratory-generated aerosol samples are created by nebulizing standard solutions of ammonium sulfate (AS, Sinopharm Chemical Reagent Co. Ltd.) and naphthalene. Then aerosol particles are impacted onto substrates using a microanalysis particle sampler. The system is shown in Figure S1. At first, air flows out of a compressor and into a two-level air filter system (0.1 and 0.01 μm, respectively) to partially remove impurities. After that, air continues into a two-level air dryer system that can remove nearly 90% percent of the moisture. This is followed by an air filter (0.01 μm) set to prevent the nebulizer from being contaminated by the remaining impurities. The nebulizer generates aerosol droplets with an aerodynamic diameter of 0.5−20 μm, whose median mass aerodynamic diameter range from 1 to 4 μm. Finally, aerosol droplets will transform into the solid phase in a chamber, in which we accelerate the dehydration by increasing the temperature to 50 °C. Individual atmospheric aerosol particles were collected on the roof of the fourth teaching building (about 20 m high) at Fudan University (121°30′ E, 31°18′ N) on the morning of April 13th, 2016. The weather was cloudy with a northeast breeze, and the real-time PM 2.5 index was 91 (data were provided by Shanghai Meteorological Bureau). The sampling site was a vertical distance of 300 m from the Handan Road, where rush hour lasts 1−2 h every weekday morning. All the samples were then collected for 1 min using a homemade microanalysis impactor, operating at a flow rate of 5 lpm. The microanalysis impactor consisted of a mini pump, a flow meter, and a sampling head.

2.2. Raman Measurement. Once impacted on quartz substrates, the aerosol particles were probed by using a XploRA confocal spectrometer (Jobin Yvon, Horiba Gr, France). The Raman scattering was excited by an external-cavity diode (785 nm) and coupled with a 100× Olympus microscope objective (Olympus, 0.90 Numerical Aperture). The instrument was calibrated against the Stokes Raman signal of pure Si at 520 cm^{-1} using a silicon wafer standard. A 600 lines per mm diffraction grating placed prior to a multichannel CCD device

DOI: 10.1021/acs.est.6b05910
Environ. Sci. Technol. 2017, 51, 6260−6267

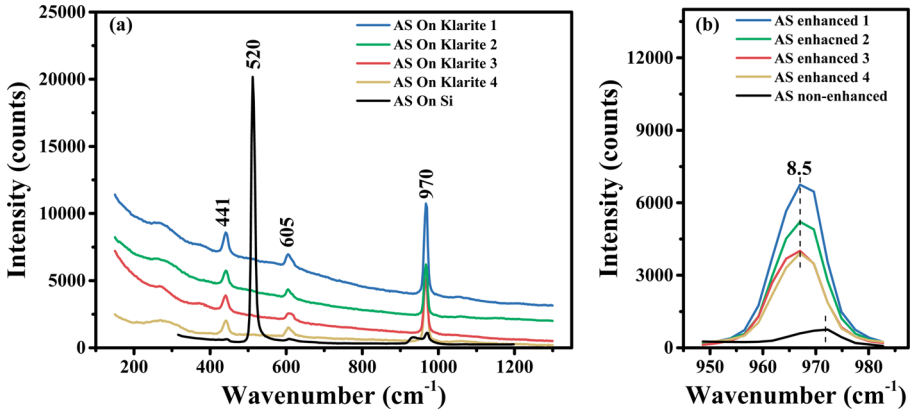

Figure 2. (a) Raman spectra of simulated AS aerosols on silicon wafer (black, averaged from five particles) and Klarite (Klarite 1, 2, 3, and 4 represent four different aerosol particles on Klarite). Klarite 4 represents a particle located outside the inverse pyramid (on the top surface of the Klarite). (b) The comparison of non-enhanced and SERS-enhanced spectra of $\nu_s(SO_4^{2-})$ at around 970 cm^{-1}. The black line represents the non-enhanced signal, and all others show an average EF of 6.1 with respect to the non-enhanced signal.

(1024 × 256 pixels) was used to collect spectra in a resolution of 3 cm^{-1}, with 10 accumulations at a 1 s acquisition time. When Raman mapping was operated, the computer-controlled Raman (*XY*) mapping automatically records nearly 900 spectra in a 30 × 30 μm^2 with 1 μm as a minimum step. To avoid damaging the aerosols, a laser power of 2 mW is used for Raman analysis.

2.3. FDTD Simulation. The experimental data was supported by a numerical simulation of the electromagnetic field using the Lumerical FDTD software. We modeled the substrate with gold[36] and etched the inverted pyramids with the same dimensions as used for the experiment. The calculation area for the finite-difference time-domain solver surrounds a single unit cell with periodic boundary conditions in the $x-y$ plane. In the z direction, we applied PML boundary conditions to model an open boundary. Due to the periodic boundary conditions applied, we simulated an infinite array illuminated by a linearly polarized plane wave, incident from 0.7 μm above the substrate surface with an amplitude of E_0 = 0.5 and a wavelength range of 500−1000 nm. A field monitor is placed in the vertical cross-section in the middle of the inverted pyramid structure to monitor the electric field (E-field) distribution.

3. RESULTS AND DISCUSSION

3.1. Enhanced Raman for Sulfate Ammonium Aerosol Particles. Ammonium sulfate (AS) is a common inorganic component in ambient aerosols whose $\nu_s(SO_4^{2-})$ is a highly Raman active mode. In this work, all of the vibrational signals are tentatively assigned on the basis of literature values, not on ab initio computations or isotopic substitution. Figure 2 shows a comparison of the non-enhanced and the SERS-enhanced spectra of the simulated (i.e., lab-made) AS aerosols. When single aerosol particles are collected on the silicon wafer (Figure 2a), they have an intense silicon signal and a weak sulfate signal due to the vibrational modes associated with the AS at 970 cm^{-1}, and the strong peak at 520 cm^{-1} is attributed to Si. On the Klarite substrate (Figure 2a), the peak intensity in the $\nu_s(SO_4^{2-})$ stretching region is significantly enhanced, and some additional minimal peaks, such as $\delta(SO_4^{2-})$ at 441 and 605 cm^{-1}, are observed as well. These can hardly be detected using the silicon substrate.[37] In Figure 2a, a dramatic enhancement due to the Klarite substrate can be seen not only for previously observed peaks but also for those that were previously below the detection limit. The size and morphology of simulated AS aerosols can be studied by scanning electron microscope (SEM). Figure S2 shows SEM images of typical AS particles with size of ~1 μm on silicon and Klarite, respectively.

To confirm the enhancement observed, we calculate the EF (enhancement factor) of the substrate. Here, EF_{SERS} is defined as the ratio of the intensity of the analyte on SERS substrate (Klarite) to that on silicon wafer, expressed in the equation: $EF_{SERS} = \frac{I_{SERS}/N_{SERS}}{I_{NRS}/N_{NRS}}$, where I_{SERS} and I_{NRS} are the SERS and normal Raman spectroscopy (NRS) intensities and N_{SERS} and N_{NRS} are the number of molecules contributing under SERS and NRS conditions, respectively.[38] In this experiment, integration times and power densities are fixed, so the data of I_{SERS} and I_{NRS} can be assumed normalized. The intensities of the peaks were calculated using peak height analysis, and baseline correction was performed before calculation. AS particles were generated and collected on Klarite and silicon wafer under identical conditions, and aerosol particles of similar size were selected and studied. The number of molecules contributing under SERS and NRS conditions are assumed to be similar. We thus calculate the EF of the peak of $\nu_s(SO_4^{2-})$ at 970 cm^{-1} and get an average EF of 6.1, with highest values of up to 8.5 (Figure 2b). Our results are larger by a factor of 3 compared to those on Ag-nanoparticle-coated substrates in the previous report.[29] This indicates the advantage of Klarite substrates possessing more uniform hotspots and stronger field enhancement. A slight shift of 5 cm^{-1} of the Raman peak is observed (Figure 2b), which is attributed to the interaction of the sample with the Klarite's gold surface, also observed in some other SERS studies.[39]

To further study the distribution for aerosol particles on the substrate, we take advantage of Raman mapping technology,[40,41] an advanced detection method of obtaining the detailed chemical image by collecting Raman signals of a specific region of the sample. The grayscale of the false-color image corresponds to the change of the Raman peaks for the parameters of concentration, distribution, molecular structure and state, stress distribution, crystallinity, etc. When we prepared nebulized aerosol particles with Klarite and silicon wafer, respectively, we got a rough understanding of the aerosols impacted on the substrates, as shown in Figure 3. On the silicon wafer, some small AS particles are observable under the microscope (Figure 3c); however, these are not detected by

DOI: 10.1021/acs.est.6b05910
Environ. Sci. Technol. 2017, 51, 6260−6267

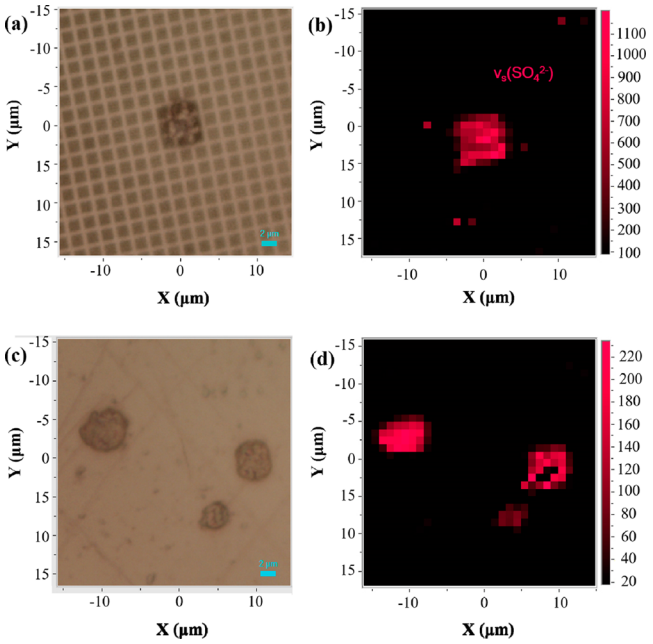

Figure 3. Microscopic image of nebulized AS aerosol particles on Klarite (a) and silicon wafer (c) and its Raman mapping image of Klarite (b) and silicon wafer (d) in the region of $\nu_s(SO_4^{2-})$.

Raman mapping (Figure 3d). On the contrary, using the Klarite substrate, not only can we detect the macroscopic particles (Figure 3a), but also, some small particles that cannot be observed under the microscope are measured with a weak signal of $\nu_s(SO_4^{2-})$ at around 970 cm^{-1} (Figure 3b). In Figure 5b,d, it is notable that the intensity of red color is related to the intensity of the Raman signal of $\nu_s(SO_4^{2-})$, and the color scale bar in Figure 3b is about 5 times more intense than that in Figure 3d. We can observe a big difference in color intensity between particles on Klarite and silicon wafers, which shows an enhancement around a factor of 5, indicating the efficient Raman enhancing effect of Klarite (Figure 3b,d). The AS particles were generated and collected on Klarite and silicon wafers under identical conditions, so the crystallinity of AS can be excluded for the enhanced Raman signal.

3.2. Enhanced Raman for Naphthalene Particles. The organic components in aerosol particles are various and exhibit high carcinogenic and mutagenic activity. Naphthalene is a white, crystalline solid and organic compound whose solubility is 19 mg/L (10 °C) in water. It is a specific type of the polycyclic aromatic hydrocarbons (PAHs) and is an ongoing concern in the atmosphere. Aerosolized NA particles are made in the same way as AS particles. The Raman spectra of the NA particles on Klarite and silicon wafer are shown in Figure 4. The Klarite substrate (Figure 4) shows a significant improvement compared to the silicon wafer. The peaks at 510 and 759 cm^{-1} are assigned to in-plane vibrations of benzene and C−C stretching. The peak at 1020 and 1576 cm^{-1} are due to C−H rocking vibrations and C−C stretching vibrations, respectively. The peak at around 1378 cm^{-1} is attributed to C−C stretching modes.[42] Similar to the previously described measurements, almost no signal of NA can be seen on the silicon wafer (the strongest peak in 520 cm^{-1} is from Si), while the Raman peak of aerosols on the Klarite is very distinct.

We also calculated the EF of the Klarite with NA particles collected on the substrate. The EF was calculated using the same method as for AS particles. As shown in Figure 4, the highest EF on Klarite is 5.5, and the average EF is 3.6. This also indicates the good performance of Klarite substrates for analyzing organic components in aerosol particles. Therefore, Klarite is a perfect complementary tool for studying the organic compositions and their distributions in an individual secondary organic aerosol and also the forming process of secondary organic aerosols.

3.3. Raman Spectra for Atmospheric Aerosols. We sampled the atmospheric aerosols at Fudan University on a cloudy day, as described previously. Figure 5 shows the point-by-point Raman mapping of the sampled aerosols in a region about 40 × 40 μm^2 on Klarite, which allows an assessment of the chemical components, such as amorphous carbon (green) around 1100−1700 cm^{-1} (Figure 5a), inorganic salt (red) around 1000 cm^{-1} (Figure 5b),[37,43] and organic compounds (yellow) around 822 cm^{-1} (Figure 5c). The peak at 1039 cm^{-1} is in agreement with the mode of $\nu(NO_3^-)$, which is extensively distributed on the substrate. We observed large areas of amorphous carbon on the substrate with a broad peak,[44] which is probably due to the morning rush hour close to the campus. These results indicate that the components of the ambient aerosols are full of nitrate and amorphous carbon, which can be assumed to be fresh and vehicle-originated.[45] As shown in Figure 5c, we can analyze a single spectrum of a set of spectra

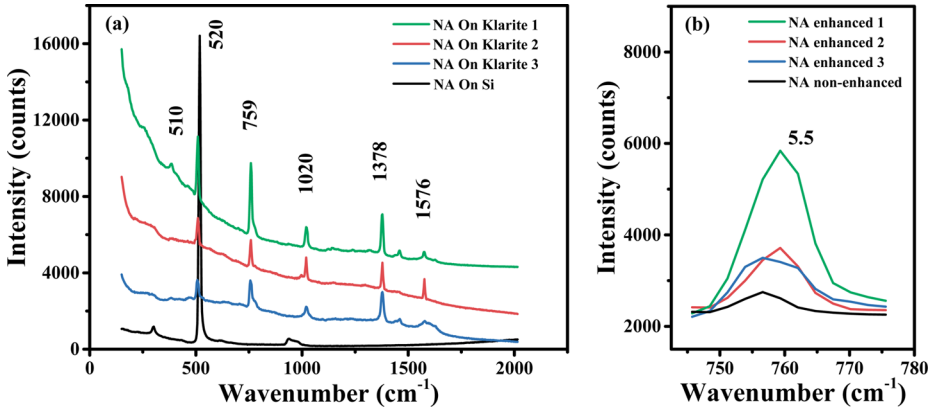

Figure 4. (a) Raman spectra of naphthalene particles on silicon wafer (black, averaged from five particles) and Klarite (Klarite 1, 2, and 3 represent three different aerosol particles). (b) The comparison of non-enhanced and SERS-enhanced spectra for the mode of C−C stretching at 759 cm^{-1}. The black line represents the non-enhanced signal, and all others show an obvious EF with respect to the non-enhanced.

DOI: 10.1021/acs.est.6b05910
Environ. Sci. Technol. 2017, 51, 6260−6267

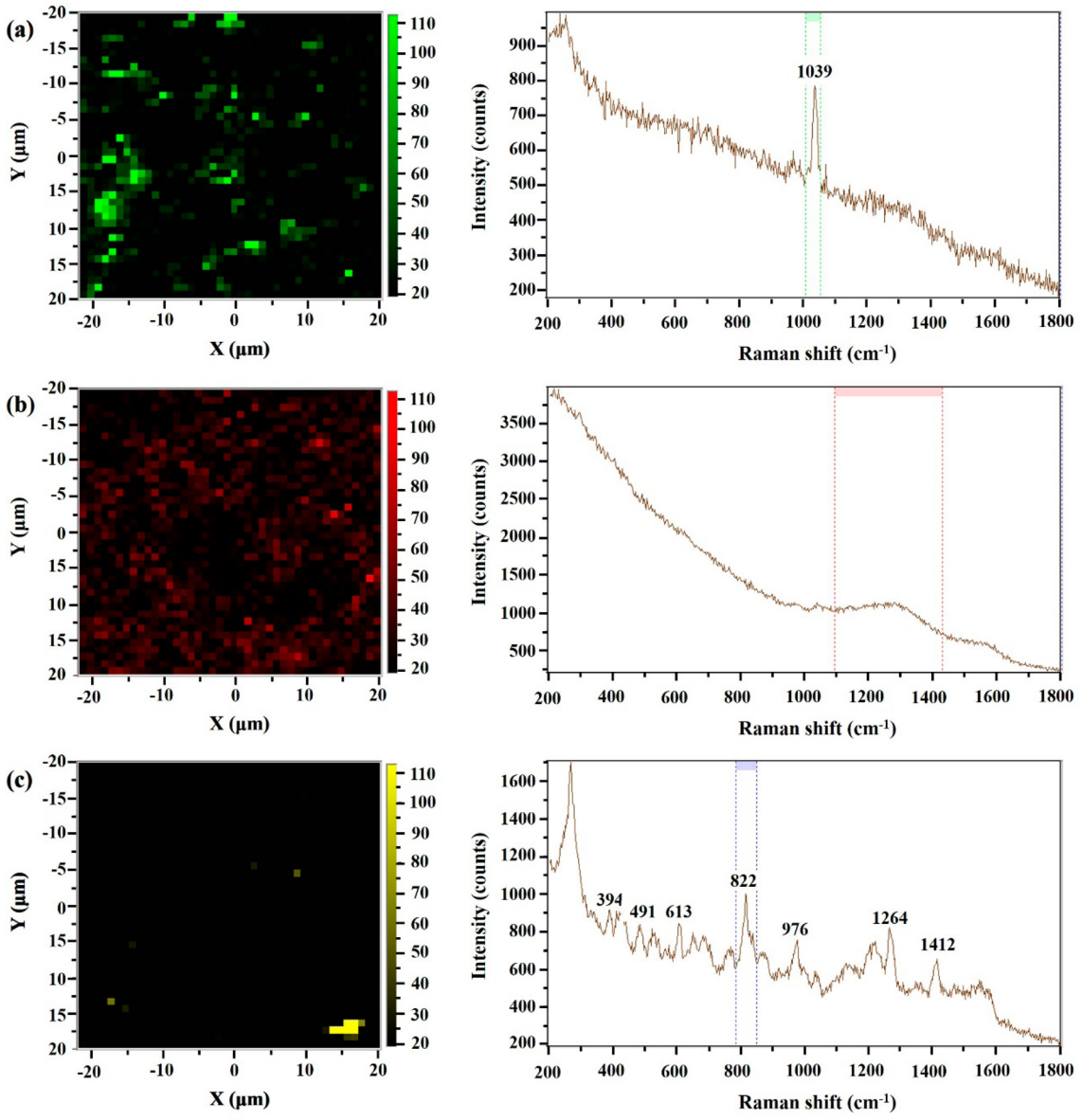

Figure 5. Raman mapping images of different functional group regions, such as inorganic salt (a), amorphous carbon (b), and organic compounds (c).

and obtain the chemical information on some specific components of interest. The yellow intensity of the spectral region represents the functional groups at 822 cm^{-1}, corresponding to symmetric ring breathing. The spectra collected also have peaks at 613, 1264, and 1412 cm^{-1}, respectively,[42,46,47] all corresponding to the ring vibration of polynuclear aromatic compounds. Therefore, aerosol pieces at this spot were likely to contain chemical substances such as anthracene, pyrene, and their derivatives. Because the molecules of PAHs contain many atoms, they contribute large numbers of fundamental vibrations. Some of them are strongly Raman active, and some are weakly Raman active.[48] SERS enables us to analyze the aerosol particles collected on the substrate more conveniently and observe more chemical information that was previously undetected. By Raman mapping, we can readily get the distribution information on chemical components of the aerosol particles. This kind of fast detection is quite useful in our daily atmospheric observation. We can get a quick Raman mapping image of chemical information in the individual aerosol particles, which might not be possible with the methods based on mass spectrometry or chromatography.

The reusability of the Klarite substrate is a critical factor for its practical application. To recycle the used Klarite substrate, we first rinsed the substrate in the ethanol with ultrasonic cleaning for 5 min followed by plasma etching for 1 h. The effect can be seen in Figure S3, showing a plain background by Raman characterization. A total of 20 sites were randomly selected on recycled Klarite for Raman mapping ananlysis (20 × 25 μm^2), and only 2 sites were slightly polluted. No aerosol particles were observable, suggesting the effectiveness of cleaning. The Raman enhancement is still apparent after 5 cycles (Figure S3). Therefore, we are confident that the ultrasonic cleaning, in addition to plasma cleaning, is effective and the substrate is reusable. The SERS intensity is closely related to EF, laser power, the effective number of molecules adsorbed or molecule orientations on metallic surface, the morphology of the substrate, and the efficiency of the optical system.[49] Because of so many influencing factors, it is difficult

DOI: 10.1021/acs.est.6b05910
Environ. Sci. Technol. 2017, 51, 6260−6267

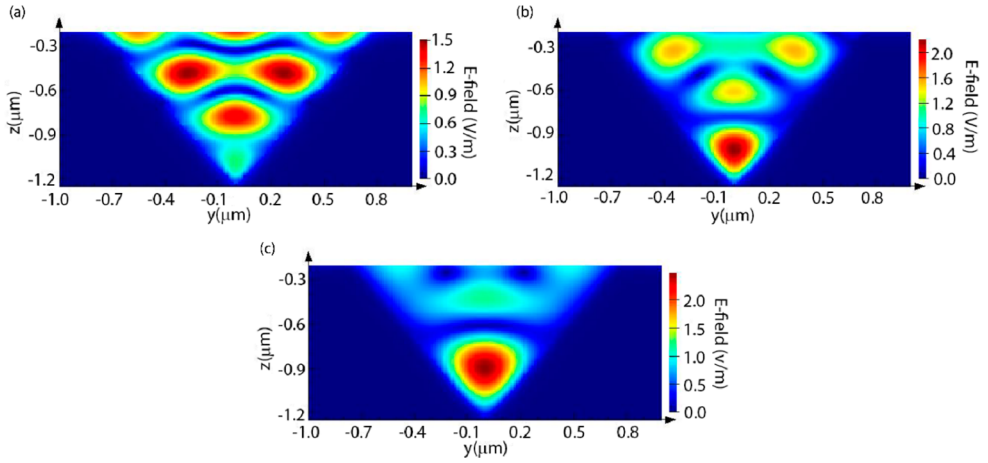

Figure 6. E-field distribution simulated for the inverted pyramid Klarite structures at 571 (a), 666 (b), and 800 nm (c) illumination, respectively.

to achieve high reproducibility of SERS. The reproducibility of Klarite for analyzing molecules has been reported to be better than 10%.[50]

3.4. FDTD Simulation of Klarite. According to the experimental results, Klarite is an effective substrate for detecting aerosol particles due to its specialized inverted-pyramid structure. To understand the mechanism and help the future design of SERS substrates for aerosol particle characterization, we thus performed electric field distribution simulations based on the finite-difference time-domain (FDTD) method. Figure 6a–c shows the E-field in the inverted pyramid Klarite structures upon illumination with 571, 666, and 800 nm light, respectively. We see that the E-field hotspots are strongly localized toward the bottom of the pit and close to the sides. For the 666 nm mode (Figure 6b), we see that the electric field is strongly localized in the lower part of the pit, with a maximum intensity of about twice that of the incident E-field of light. This enhancement is in agreement with the 8-fold enhancements observed in the experimental results. Hence, the large experimental enhancement of Raman signal that we observed can be attributed directly to the enhancement and the location of the optical near-field hotspots. Klarite allows the resonances to be tuned to two commonly used Raman excitations at 785 and 633 nm. We highlight the reliability and reproducibility of the SERS enhancement from one aerosol particle to another. This precise and reproducible nature of the substrate ensures the reliability of the experimental results. For aerosol particles, the pits of the substrate provide a normalized metric, as well as a good enhancement and reproducibility, which are all very useful for researchers studying the components of aerosols. The results also provide the direction to design efficient SERS substrate for studying atmospheric aerosols.

Compared to other research on SERS, reporting an EF of >100, the main difference of this work is the choice of the analyte used. In our case, aerosol particle sizes of several micrometers are studied by SERS, which is substantially different to those studying the Raman enhancement of molecules on the substrate. First, direct chemical interaction between the analyzed molecules and the substrate is an important reason for the high EF. In this work, only the molecules on the interface of the aerosol and substrate have a direct contact with the substrate. Second, due to the large size of the aerosol, only part of Raman scattering of the aerosol is affected by the enhanced E-field of the substrate, and the average EF is thus low. However, the EF reported here is higher than in other works focusing on individual aerosol particles using self-assembled Ag nanoparticles as the substrate.[29]

Due to the inverse pyramid shape of the Klarite substrate, the morphology of the aerosols may also affect the Raman enhancement. Some long rodlike aerosols or fractal-shaped aerosols cannot enter the cavity and access the high-field-enhancement region, while smaller spherical particles can easily access the inside of the inverse pyramid. It is difficult to control the morphology of the aerosol in this study; instead, we investigated some aerosols that were located outside the inverse pyramid (on the top surface of Klarite). In Figure 2, the Raman signal is also enhanced (AS enhanced 4), but the EF is slightly smaller than those obtained for the aerosols located inside the cavity, as expected.

4. OVERVIEW AND FUTURE WORK

SERS is demonstrated to be a promising approach for detecting the chemical components in aerosol particles. In previous research on aerosol particles, gas chromatography (GC) and mass spectrometry were widely utilized. The GC method is capable of precisely measuring the concentrations of gaseous organic compounds. The ATOFMS–SPAMS method is proficient in analyzing the species and concentrations of single aerosol particles. SERS can be a good supplementary tool for the aerosol particle research. For a simulated single aerosol particle, a significant enhancement from the Klarite is beneficial to making a qualitative analysis, even if the sample is of relatively low concentration (that is, Klarite can improve the detection limit). For SERS measurements, the sampling time can be very short, and pretreatment of the samples is not necessary; a few minutes are enough to collect sporadic and nonaggregated individual particles. However, the traditional analytical methods, such as GC, liquid chromatography, and mass spectroscopy usually need long-time field sampling for the bulk analysis and complicated sample pretreatment processes. For real-time atmospheric aerosols, SERS is a facile, efficient, and reproducible method. Additionally, it has great potential for providing a considerably more accurate analysis of the chemical components in just about 1 min.

However, there are still some challenges in applying SERS for single aerosol particle detection. First, even for SERS spectra collected with high spectral resolution, the Raman shifted peaks can overlap with each other in the case of highly

DOI: 10.1021/acs.est.6b05910
Environ. Sci. Technol. 2017, 51, 6260–6267

concentrated components. Also, a disadvantage is that different organic functional groups containing the same bond cannot be differentiated in the Raman spectra. Moreover, the quantitative analysis and sometimes even qualitative observations of single aerosol particles (especially tracing organic functional groups in ambient aerosols) with SERS are still constrained to a large extent. However, for a single vibrational mode, it is possible to make a quantitative analysis. For tracing and multicomponent aerosol particles, it is much harder and more sophisticated to make a quantitative rather than a semiquantitative analysis. The inhomogeneous character of the aerosols can also affect the SERS measurement, as the parts that are placed in the field enhancement region are preferentially sampled. To address these challenges, we may combine SERS with another analysis method to obtain a more-complete understanding of an individual aerosol particle. Examples of such methods are energy-dispersive X-ray, infrared spectroscopic, or atomic force microscopy.[51] Meanwhile, the fabrication of Klarite is quite important as it is a well-ordered, precisely structured, and mature substrate. All of these characteristics are necessary for achieving reproducible and strong spectra of the aerosol particles. Research on developing SERS substrates with good reproducibility and enhancement effects will be a critical part in our future work. Undoubtedly, SERS will be a necessary complement to the mass-spectrometry-based analysis of aerosols, which is capable of analyzing the species within individual aerosol particles from both the lab and the ambient atmosphere.

■ ASSOCIATED CONTENT

Supporting Information

The Supporting Information is available free of charge on the ACS Publications website at DOI: 10.1021/acs.est.6b05910.

Figures showing a schematic diagram of the experimental system for nebulizing simulated aerosols, SEM images, the mapping of plain substrate, and Raman spectra. (PDF)

■ AUTHOR INFORMATION

Corresponding Author

*Phone and fax: 86-21-6564-2781; e-mail: zhanglw@fudan.edu.cn.

ORCID

Liwu Zhang: 0000-0002-0765-8660

Notes

The authors declare no competing financial interest.

■ ACKNOWLEDGMENTS

The authors gratefully acknowledge financial support from National Natural Science Foundation of China (grant nos. 21507011 and 21677037), the Ministry of Science and Technology of the People's Republic of China (grant nos. 2016YFE0112200 and 2016YFC0203700), and Marie Skłodowska-Curie Actions (grant no. 690958-MARSU-RISE-2015).

■ REFERENCES

(1) Gao, Y.; Anderson, J. R. Characteristics of Chinese aerosols determined by individual-particle analysis. *Journal of Geophysical Research: Atmospheres.* **2001**, *106*, 18037−18045.

(2) McFiggans, G.; Artaxo, P.; Baltensperger, U.; Coe, H.; Facchini, M. C.; Feingold, G.; Fuzzi, S.; Gysel, M.; Laaksonen, A.; Lohmann, U.; et al. The effect of physical and chemical aerosol properties on warm cloud droplet activation. *Atmos. Chem. Phys.* **2006**, *6*, 2593−2649.

(3) Hallquist, M.; Wenger, J.; Baltensperger, U.; Rudich, Y.; Simpson, D.; Claeys, M.; Dommen, J.; Donahue, N.; George, C.; Goldstein, A.; et al. The formation, properties and impact of secondary organic aerosol: current and emerging issues. *Atmospheric Chemistry and Physics.* **2009**, *9*, 5155−5236.

(4) Chan, L. P.; Chan, C. K. Role of the aerosol phase state in ammonia/amines exchange reactions. *Environ. Sci. Technol.* **2013**, *47*, 5755−5762.

(5) De Bock, L. A.; Van Malderen, H.; Van Grieken, R. E. Individual aerosol particle composition variations in air masses crossing the north sea. *Environ. Sci. Technol.* **1994**, *28*, 1513−1520.

(6) Gard, E.; Mayer, J. E.; Morrical, B. D.; Dienes, T.; Fergenson, D. P.; Prather, K. A. Real-time analysis of individual atmospheric aerosol particles: Design and performance of a portable ATOFMS. *Anal. Chem.* **1997**, *69*, 4083−4091.

(7) Li, W.; Shao, L.; Zhang, D.; Ro, C.-U.; Hu, M.; Bi, X.; Geng, H.; Matsuki, A.; Niu, H.; Chen, J. A review of single aerosol particle studies in the atmosphere of East Asia: morphology, mixing state, source, and heterogeneous reactions. *J. Cleaner Prod.* **2016**, *112*, 1330−1349.

(8) Krieger, U. K.; Marcolli, C.; Reid, J. P. Exploring the complexity of aerosol particle properties and processes using single particle techniques. *Chem. Soc. Rev.* **2012**, *41*, 6631−6662.

(9) Surratt, J. D.; Gomez-Gonzalez, Y.; Chan, A. W.; Vermeylen, R.; Shahgholi, M.; Kleindienst, T. E.; Edney, E. O.; Offenberg, J. H.; Lewandowski, M.; Jaoui, M.; Maenhaut, W.; Claeys, M.; Flagan, R. C.; Seinfeld, J. H. Organosulfate formation in biogenic secondary organic aerosol. *J. Phys. Chem. A* **2008**, *112*, 8345−8378.

(10) Ault, A. P.; Axson, J. L. Atmospheric Aerosol Chemistry: Spectroscopic and Microscopic Advances. *Anal. Chem.* **2017**, *89*, 430−452.

(11) Chu, Y.; Sauerwein, M.; Chan, C. K. Hygroscopic and phase transition properties of alkyl aminium sulfates at low relative humidities. *Phys. Chem. Chem. Phys.* **2015**, *17*, 19789−19796.

(12) Jordanov, N.; Zellner, R. Investigations of the hygroscopic properties of ammonium sulfate and mixed ammonium sulfate and glutaric acid micro droplets by means of optical levitation and Raman spectroscopy. *Phys. Chem. Chem. Phys.* **2006**, *8*, 2759−2764.

(13) Ault, A. P.; Guasco, T. L.; Baltrusaitis, J.; Ryder, O. S.; Trueblood, J. V.; Collins, D. B.; Ruppel, M. J.; Cuadra-Rodriguez, L. A.; Prather, K. A.; Grassian, V. H. Heterogeneous Reactivity of Nitric Acid with Nascent Sea Spray Aerosol: Large Differences Observed between and within Individual Particles. *J. Phys. Chem. Lett.* **2014**, *5*, 2493−2500.

(14) Cai, C.; Stewart, D. J.; Reid, J. P.; Zhang, Y. H.; Ohm, P.; Dutcher, C. S.; Clegg, S. L. Organic component vapor pressures and hygroscopicities of aqueous aerosol measured by optical tweezers. *J. Phys. Chem. A* **2015**, *119*, 704−718.

(15) Cotterell, M. I.; Mason, B. J.; Preston, T. C.; Orr-Ewing, A. J.; Reid, J. P. Optical extinction efficiency measurements on fine and accumulation mode aerosol using single particle cavity ring-down spectroscopy. *Phys. Chem. Chem. Phys.* **2015**, *17*, 15843−15856.

(16) Takahama, S.; Gilardoni, S.; Russell, L. M.; Kilcoyne, A. L. D. Classification of multiple types of organic carbon composition in atmospheric particles by scanning transmission X-ray microscopy analysis. *Atmos. Environ.* **2007**, *41*, 9435−9451.

(17) Nie, S.; Emory, S. R. Probing Single Molecules and Single Nanoparticles by Surface-Enhanced Raman Scattering. *Science* **1997**, *275*, 1102−1106.

(18) Jiao, Y.; Ryckman, J. D.; Ciesielski, P. N.; Escobar, C. A.; Jennings, G. K.; Weiss, S. M. Patterned nanoporous gold as an effective SERS template. *Nanotechnology* **2011**, *22*, 295302.

(19) Baker, G. A.; Moore, D. S. Progress in plasmonic engineering of surface-enhanced Raman-scattering substrates toward ultra-trace analysis. *Anal. Bioanal. Chem.* **2005**, *382*, 1751−1770.

(20) Aggarwal, R. L.; Di Cecca, S.; Farrar, L. W.; Shabshelowitz, A.; Jeys, T. H. Sensitive Detection and Identification of Isovanillin Aerosol

DOI: 10.1021/acs.est.6b05910
Environ. Sci. Technol. 2017, 51, 6260−6267

Particles at the pg/cm3Mass Concentration Level Using Raman Spectroscopy. *Aerosol Sci. Technol.* **2015**, *49*, 753−756.
(21) Schlucker, S. Surface-enhanced Raman spectroscopy: concepts and chemical applications. *Angew. Chem., Int. Ed.* **2014**, *53*, 4756−4795.
(22) Stiles, P. L.; Dieringer, J. A.; Shah, N. C.; Van Duyne, R. P. Surface-enhanced Raman spectroscopy. *Annu. Rev. Anal. Chem.* **2008**, *1*, 601−626.
(23) Gao, Q.; Zhao, A.; Gan, Z.; Tao, W.; Li, D.; Zhang, M.; Guo, H.; Wang, D.; Sun, H.; Mao, R. Facile fabrication and growth mechanism of 3D flower-like Fe 3 O 4 nanostructures and their application as SERS substrates. *CrystEngComm.* **2012**, *14*, 4834−4842.
(24) Shanmukh, S.; Jones, L.; Driskell, J.; Zhao, Y.; Dluhy, R.; Tripp, R. A. Rapid and sensitive detection of respiratory virus molecular signatures using a silver nanorod array SERS substrate. *Nano Lett.* **2006**, *6*, 2630−2636.
(25) Liu, G. L.; Lee, L. P. Nanowell surface enhanced Raman scattering arrays fabricated by soft-lithography for label-free biomolecular detections in integrated microfluidics. *Appl. Phys. Lett.* **2005**, *87*, 074101.
(26) Yan, B.; Thubagere, A.; Premasiri, W. R.; Ziegler, L. D.; Dal Negro, L.; Reinhard, B. M. Engineered SERS substrates with multiscale signal enhancement: nanoparticle cluster arrays. *ACS Nano* **2009**, *3*, 1190−1202.
(27) Brown, R. J.; Milton, M. J. Nanostructures and nanostructured substrates for surface—enhanced Raman scattering (SERS). *J. Raman Spectrosc.* **2008**, *39*, 1313−1326.
(28) Ayora, M. J.; Ballesteros, L.; Perez, R.; Ruperez, A.; Laserna, J. J. Detection of atmospheric contaminants in aerosols by surface-enhanced Raman spectrometry. *Anal. Chim. Acta* **1997**, *355*, 15−21.
(29) Craig, R. L.; Bondy, A. L.; Ault, A. P. Surface Enhanced Raman Spectroscopy Enables Observations of Previously Undetectable Secondary Organic Aerosol Components at the Individual Particle Level. *Anal. Chem.* **2015**, *87*, 7510−7514.
(30) Sengupta, A.; Laucks, M. L.; Dildine, N.; Drapala, E.; Davis, E. J. Bioaerosol characterization by surface-enhanced Raman spectroscopy (SERS). *J. Aerosol Sci.* **2005**, *36*, 651−664.
(31) Sengupta, A.; Brar, N.; Davis, E. J. Bioaerosol detection and characterization by surface-enhanced Raman spectroscopy. *J. Colloid Interface Sci.* **2007**, *309*, 36−43.
(32) Botti, S.; Cantarini, L.; Almaviva, S.; Puiu, A.; Rufoloni, A. Assessment of SERS activity and enhancement factors for highly sensitive gold coated substrates probed with explosive molecules. *Chem. Phys. Lett.* **2014**, *592*, 277−281.
(33) Craig, A. P.; Franca, A. S.; Irudayaraj, J. Surface-enhanced Raman spectroscopy applied to food safety. *Annu. Rev. Food Sci. Technol.* **2013**, *4*, 369−380.
(34) Zheng, J.; He, L. Surface-Enhanced Raman Spectroscopy for the Chemical Analysis of Food. *Compr. Rev. Food Sci. Food Saf.* **2014**, *13*, 317−328.
(35) Gajaraj, S.; Fan, C.; Lin, M.; Hu, Z. Quantitative detection of nitrate in water and wastewater by surface-enhanced Raman spectroscopy. *Environ. Monit. Assess.* **2013**, *185*, 5673−5681.
(36) Palik, E. D. *Handbook of Optical Constants of Solids*; Academic Press: New York, 1985; Vol. *3*.
(37) Zhang, Y.-H.; Chan, C. K. Understanding the hygroscopic properties of supersaturated droplets of metal and ammonium sulfate solutions using Raman spectroscopy. *J. Phys. Chem. A* **2002**, *106*, 285−292.
(38) Kleinman, S. L.; Frontiera, R. R.; Henry, A. I.; Dieringer, J. A.; Van Duyne, R. P. Creating, characterizing, and controlling chemistry with SERS hot spots. *Phys. Chem. Chem. Phys.* **2013**, *15*, 21−36.
(39) Fleger, Y.; Mastai, Y.; Rosenbluh, M.; Dressler, D. H. SERS as a probe for adsorbate orientation on silver nanoclusters. *J. Raman Spectrosc.* **2009**, *40*, 1572−1577.
(40) Batonneau, Y.; Sobanska, S.; Laureyns, J.; Bremard, C. Confocal microprobe Raman imaging of urban tropospheric aerosol particles. *Environ. Sci. Technol.* **2006**, *40*, 1300−1306.
(41) Sobanska, S.; Falgayrac, G.; Laureyns, J.; Brémard, C. Chemistry at level of individual aerosol particle using multivariate curve resolution of confocal Raman image. *Spectrochim. Acta, Part A* **2006**, *64*, 1102−1109.
(42) Shinohara, H.; Yamakita, Y.; Ohno, K. Raman spectra of polycyclic aromatic hydrocarbons. Comparison of calculated Raman intensity distributions with observed spectra for naphthalene, anthracene, pyrene, and perylene. *J. Mol. Struct.* **1998**, *442*, 221−234.
(43) Nyquist, R. A.; Kagel, R. O. *Handbook of Infrared and Raman Spectra of Inorganic Compounds and Organic Salts: Infrared Spectra of Inorganic Compounds*; Academic Press: New York, 2012; Vol. *4*.
(44) Ferrari, A. C.; Robertson, J. Interpretation of Raman spectra of disordered and amorphous carbon. *Phys. Rev. B: Condens. Matter Mater. Phys.* **2000**, *61*, 14095−14107.
(45) Ivleva, N. P.; Messerer, A.; Yang, X.; Niessner, R.; Poschl, U. Raman microspectroscopic analysis of changes in the chemical structure and reactivity of soot in a diesel exhaust aftertreatment model system. *Environ. Sci. Technol.* **2007**, *41*, 3702−3707.
(46) Asher, S. A. Ultraviolet resonance Raman spectrometry for detection and speciation of trace polycyclic aromatic hydrocarbons. *Anal. Chem.* **1984**, *56*, 720−724.
(47) Lin-Vien, D.; Colthup, N. B.; Fateley, W. G.; Grasselli, J. G. *The Handbook of Infrared and Raman Characteristic Frequencies of Organic Molecules*; Academic Press: San Diego, CA, 1991.
(48) Suzuki, M.; Yokoyama, T.; Ito, M. Polarized Raman spectra of naphthalene and anthracene single crystals. *Spectrochimica Acta Part A: Molecular Spectroscopy* **1968**, *24*, 1091−1107.
(49) Xiong, M.; Ye, J. Reproducibility in surface-enhanced Raman spectroscopy. *Journal of Shanghai Jiaotong University (Science)* **2014**, *19*, 681−690.
(50) Perney, N. M.; Baumberg, J. J.; Zoorob, M. E.; Charlton, M. D.; Mahnkopf, S.; Netti, C. M. Tuning localized plasmons in nanostructured substrates for surface-enhanced Raman scattering. *Opt. Express* **2006**, *14*, 847−857.
(51) Ofner, J.; Deckert-Gaudig, T.; Kamilli, K. A.; Held, A.; Lohninger, H.; Deckert, V.; Lendl, B. Tip-Enhanced Raman Spectroscopy of Atmospherically Relevant Aerosol Nanoparticles. *Anal. Chem.* **2016**, *88*, 9766−9772.

DOI: 10.1021/acs.est.6b05910
Environ. Sci. Technol. 2017, 51, 6260−6267